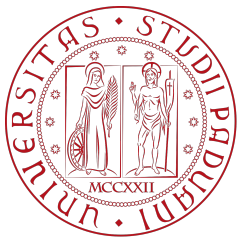

UNIVERSITÀ DEGLI STUDI DI PADOVA

Dipartimento di Fisica e Astronomia "Galileo Galilei"

Corso di Laurea in Fisica

Tesi di Laurea

Robustezza dell'entanglement in sistemi quantistici aperti a molti corpi all'infuori dell'equilibrio

Robustness of entanglement in open quantum many-body systems out of equilibrium

Relatore

Prof. Pietro Silvi

Correlatore

Dr. Darvin Wanisch

Laureando

Davide Toniato

Anno Accademico 2024/2025

Abstract (Italian)

L'entanglement è una risorsa fondamentale per le tecnologie quantistiche e svolge un ruolo cruciale nella classificazione di sistemi quantistici complessi a molti corpi. Con il rapido progresso delle tecnologie quantistiche, sta diventando sempre più fattibile ingegnerizzare e studiare tali sistemi in laboratorio. Tuttavia, i dispositivi quantistici attuali sono intrinsecamente rumorosi, e i sistemi di interesse sono inevitabilmente soggetti a dissipazione, un effetto generalmente considerato dannoso per l'entanglement. Comprendere l'interazione tra entanglement e dissipazione è essenziale per individuare i potenziali limiti dei dispositivi quantistici attuali e per guidare lo sviluppo di tecnologie quantistiche più robuste. In questa tesi esploriamo tale interazione simulando numericamente sistemi quantistici a molti corpi soggetti a dissipazione. Ci concentriamo sul modello XXZ e analizziamo l'impatto delle simmetrie sull'entanglement, sia nella dinamica transitoria successiva a un quench quantistico, sia nello stato stazionario.

Abstract (English)

Entanglement is a fundamental resource for quantum technologies and plays a crucial role in the classification of complex quantum many-body systems. As quantum technologies continue to advance rapidly, it is becoming increasingly feasible to engineer and investigate such systems in the laboratory. However, today's quantum devices are inherently noisy, and the systems of interest are inevitably subject to dissipation, which is generally regarded as harmful to entanglement. Gaining insight into the interplay between entanglement and dissipation is essential for identifying potential limitations of current quantum devices and for guiding the development of more robust quantum technologies. In this thesis, we explore this interplay by numerically simulating quantum many-body systems subject to dissipation. We focus on the XXZ model and investigate the impact of symmetries on entanglement, both during the transient dynamics following a quantum quench and in the stationary state.

Acknowledgements

First and foremost, I would like to thank Dr. Darvin Wanisch for introducing me to this exciting field of quantum information theory and for generously sharing with me the knowledge necessary not only to complete this thesis, but also to shape me into a better future physicist. I am also deeply grateful to Prof. Pietro Silvi and to the entire Quantum Group of the Department of Physics for giving me the opportunity to work alongside such talented researchers. A heartfelt thank goes to my parents and all my close relatives for providing me with love, encouragement, and support, both material and immaterial, that have sustained me throughout my academic journey. A special thanks goes to my mother, who has always listened to me, stood by my side, and reminded me to follow my dreams with courage. Last but certainly not least, I want to thank all my friends, who have supported and motivated me to always give my best. Grazie.

Contents

Chapter 1

Introduction

Entanglement is one of the most profound and distinctive features of quantum mechanics, with a central role in the understanding and classification of complex quantum systems. Moreover, it has proven to be a key resource in both quantum information theory and quantum computing, enabling important advantages in tasks such as secure key distribution and encryption. However, in its early days, entanglement was the subject of intense debate, most notably in the controversy between Albert Einstein and the proponents of the Copenhagen interpretation of quantum mechanics. Although Einstein was one the founders of this theory, he strongly rejected the idea that the quantum world is governed by indeterministic laws. His well-known remark, *'God does not play dice with the universe"*, reflects this conviction. In 1935, together with Podolsky and Rosen, Einstein published the paper *"Can Quantum-Mechanical Description of Physical Reality Be Considered Complete?"* [1]. In this work, they argued that quantum mechanics only appears to be non-deterministic because its formulation is incomplete. Einstein argued that a complete physical theory must assign a theoretical counterpart to every element of reality, which he defined as any physical quantity whose value can be predicted with certainty without disturbing the system. Building on this definition, Einstein, Podolsky, and Rosen noted that in quantum mechanics two non-commuting observables cannot both be assigned definite values simultaneously: measuring one determines its value but precludes precise knowledge of the other, as described by the Heisenberg uncertainty principle. From this they concluded that either quantum mechanics is incomplete, or two non-commuting observables cannot correspond to simultaneous elements of reality. To exclude the second conclusion, they considered two subsystems, A and B, which interacted with each other before being separated. A measurement of an observable on subsystem A collapses the system's wavefunction, thereby fixing the corresponding value on B. The same occurs for a different, non-commuting observable. Since A and B no longer interact, no actual change can take place in B as a result of actions on A. Therefore, two non-commuting observables can be regarded as simultaneous elements of reality, which cannot both be described by the collapsed wavefunction, implying that the quantum-mechanical description is not complete.

Following this publication, later known as the EPR paradox, Schrödinger responded with another paper entitled *'Discussion of Probability Relations between Separated Systems"* [2], where, instead of trying to prove Einstein, Podolsky and Rosen wrong, he formalized the properties of separated systems and introduced the concept of *entanglement*. With respect to this phenomenon, he famously remarked: *"I would not call that one but rather the characteristic trait of quantum mechanics, the one that enforces its entire departure from classical lines of thought."* Schrödinger emphasized that the best possible knowledge of the whole system does not necessarily imply the best possible knowledge of its parts. This limitation, he argued, arises not from incomplete information, but from the very presence of an interaction that generates non-local correlations between subsystems. Einstein recognized that even the principle of locality, which asserts that an object can be directly influenced only by its immediate surroundings and that distant actions cannot propagate instantaneously but only at a finite speed, was undermined. Faced with this unsettling implication, he famously referred to entanglement as *"spooky action at a distance."* He remained convinced that a local deterministic theory was required, since the

apparent randomness of quantum mechanics could not, in his view, be fundamental.

This conviction foreshadowed the later development of hidden-variable theories, which are based on the hypothesis that local parameters, not necessarily measurable, can be introduced to reproduce the results of quantum mechanics while preserving determinism. One of the most influential examples was developed in 1952 by David Bohm [3], who refined the earlier idea of pilot waves originally proposed by Louis de Broglie. However, Bohm's formulation relied on the presence of non-local quantum potentials, thereby violating the principle of locality.

In 1964, thirty years after the EPR paradox, John S. Bell reconsidered the problem of entanglement, by then largely neglected, and published his groundbreaking paper *"On the Einstein Podolsky Rosen Paradox"* [4]. From this work originated a series of results [5], which demonstrated that certain inequalities, now known as *Bell's inequalities*, must hold in any local hidden-variable theory. Quantum mechanics, however, predicts situations in which these inequalities are violated. Therefore, if experiments confirm such violations, non-local correlations, such as those originated from entanglement, must exist. Over the following decades, numerous experiments [6–11] tested Bell's inequalities, progressively addressing potential loopholes and refining the methodology. This line of research culminated in 2022, when the Nobel Prize in Physics was awarded to Alain Aspect, John Clauser, and Anton Zeilinger *"for experiments with entangled photons, establishing the violation of Bell inequalities and pioneering quantum information science."* Although non-local hidden-variable theories remain a logical possibility, no formulation developed so far can match the predictive power and internal consistency of quantum mechanics. Moreover, extending hidden-variable models to relativity has proven to be extremely challenging, further limiting their role as alternatives to standard quantum mechanics.

After first experimental tests in the 1970s demonstrating the violation of Bell's inequalities, it became clear that entanglement is a fundamental feature of the quantum world. Nevertheless, its significance remained uncertain until the mid-1990s, when it was formally quantified through the introduction of the first entanglement measures. As expressed by the Horodecki family in their 2007 review article *"Quantum Entanglement"* [12]: *"It has become clear that entanglement is not only a subject of philosophical debates, but it is a new quantum resource for tasks which cannot be performed by means of classical resources. It can be manipulated, broadcast, controlled, and distributed."* Today, entanglement lies at the foundation of many key advances in quantum technologies, including quantum cryptography based on Bell's theorem, quantum key distribution [13], quantum dense coding [14], quantum teleportation [15], and, more generally, quantum computation [16–19]. In all these protocols, entanglement acts as a resource, which can be consumed to perform operations that are otherwise impossible for classical systems.

Unfortunately, quantum entanglement is highly fragile, as even in the simplest systems, a weak interaction with the environment is sufficient to cause this resource to decay. Despite efforts to isolate quantum systems and engineer ideal conditions, modern quantum technologies remain inherently noisy. The coupling of a physical system to its environment can induce *decoherence*, a process that suppresses quantum superpositions and destroys entanglement. Over time, this leads to a loss of information about the system's quantum state, which effectively becomes indistinguishable from a classical statistical mixture. In other words, once quantum correlations vanish, the system behaves as a purely classical one, and the aforementioned advantages of quantum mechanics are completely lost. It is therefore of fundamental importance to study entanglement in the presence of dissipation and to explore mechanisms by which its complete decay can be avoided.

Recent studies have shown that, by exploiting symmetry constraints in the dynamics of open quantum systems, it is possible for such systems to relax into non-trivial stationary states. In this case, dissipation does not simply drive the system toward complete thermalization with its environment, but instead preserves a fraction of its initial quantum information. In particular, a recent paper published in 2025 by Pollmann *et al.*, titled *"Highly entangled stationary states from strong symmetries"* [20], demonstrates that when a strong non-Abelian symmetry, such as SU(2), is present, the dynamics can give rise to entangled stationary states. This implies that, despite the unavoidable presence of noise, part of the system's entanglement can persist indefinitely, enabling a consistent and robust use of this

resource in quantum protocols.

Building on these ideas, the aim of this thesis is to study entanglement dynamics in open quantum many-body systems, through numerical simulations of one-dimensional lattices of interacting qubits. Our analysis will include a complete characterization of bipartite entanglement, introducing key measures such as the von Neumann entropy, the entanglement of formation, and the logarithmic negativity. In Chapter 2 we will present the theoretical foundations of these measures and provide an informational interpretation of the corresponding formalism. Moreover, in Chapter 3 we will investigate the dynamics of open quantum systems within the Lindblad formalism, which extends the Schrödinger equation to incorporate dissipation and decoherence. Finally, in Chapter 4 we will examine entanglement dynamics following a quantum quench governed by the XXZ Hamiltonian in the presence of various dissipation channels arising from environmental interactions. In particular, in Sec. 3.2 we will analyze how symmetries shape the system's evolution and influence entanglement behavior at long times.

Although one-dimensional systems of interacting qubits represent one of the simplest quantum many-body models, they already offer valuable insights into the generic behavior of complex quantum systems. At the same time, they are highly relevant in practice, as they can be realized and explored on current quantum simulation platforms [21–25]. The ability to control and stabilize entanglement in such settings is therefore of fundamental importance for the development of future quantum technologies. More generally, the challenge of understanding systems that are intrinsically quantum mechanical yet analytically insolvable lies at the frontier of modern physics. The exponential growth of computational complexity with system size makes classical simulation of quantum dynamics impractical. This observation led Richard Feynman, in his seminal 1982 lecture *"Simulating physics with computers"* [17], to remark: *"Nature isn't classical, dammit, and if you want to make a simulation of nature, you'd better make it quantum mechanical."* His proposition anticipated the central idea that the future of physics itself crucially depends on our ability to control quantum technologies not merely as tools for computation, but as the only viable path toward uncovering the laws that govern the most complex phenomena of the universe.

Chapter 2

Entanglement in quantum many-body systems

In this chapter, we address the problem of characterizing and quantifying entanglement in quantum many-body systems. In particular we focus on quantum lattice models, i.e. systems defined on a spatial lattice, where each lattice site is associated with a two-level system, namely a qubit. A lattice composed of N sites thus corresponds to a Hilbert space $\mathcal{H}$ of dimension $D = 2^N$. More specifically, we are interested in studying the correlations for a bipartition of such lattices into two subsystems, A and B. Denoting the cardinalities of the subsystems, i.e. the number of sites contained in each of them, by $|A|$ and $|B|$ respectively, and assuming without loss of generality that $|A| \leq |B|$, the dimensions of the local Hilbert spaces $\mathcal{H}_A$ and $\mathcal{H}_B$ are given by $D_A = 2^{|A|}$ and $D_B = 2^{|B|}$.

2.1 Pure states

A system as described above, if isolated from its environment, can be represented by a *pure state* $|\psi\rangle$, which is an element of the global Hilbert space $\mathcal{H}$ and encodes maximal knowledge about the system's state. Let us consider a single qubit, whose measurement yields only two possible outcomes, typically labeled 0 and 1, analogous to a classical bit of information. The corresponding Hilbert space is $\mathbb{C}^2$, and any of its pure states can be expressed as linear combinations of two linearly independent vectors. A common choice is the computational basis, consisting of the eigenvectors of the third Pauli matrix $Z = \mathrm{diag}(1, -1)$:

$$|0\rangle = \begin{pmatrix} 1 \\ 0 \end{pmatrix} \qquad |1\rangle = \begin{pmatrix} 0 \\ 1 \end{pmatrix} .$$

Considering now a lattice of N sites, its Hilbert space $\mathcal{H}$ is given by the tensor product of the local Hilbert spaces associated with the individual qubits. The simplest example is a system of two qubits, whose Hilbert space is $\mathcal{H} = \mathcal{H}_A \otimes \mathcal{H}_B$, spanned by the tensor products of the computational basis vectors of each qubit:

$$\begin{aligned} |00\rangle = |0\rangle_A \otimes |0\rangle_B &= \begin{pmatrix} 1 & 0 & 0 & 0 \end{pmatrix}^T & |01\rangle = |0\rangle_A \otimes |1\rangle_B &= \begin{pmatrix} 0 & 1 & 0 & 0 \end{pmatrix}^T \\ |10\rangle = |1\rangle_A \otimes |0\rangle_B &= \begin{pmatrix} 0 & 0 & 1 & 0 \end{pmatrix}^T & |11\rangle = |1\rangle_A \otimes |1\rangle_B &= \begin{pmatrix} 0 & 0 & 0 & 1 \end{pmatrix}^T . \end{aligned}$$

Many-body systems are considerably more challenging to analyze than a single qubit. As mentioned in the first paragraph, the dimension of the Hilbert space $\mathcal{H}$ scales exponentially with the number of lattice sites, and even relatively small systems require enormous computational resources for their simulation. For instance, the state of a system composed of 30 qubits is represented by a D-dimensional array, whose entries are complex numbers. In Python, each complex number is typically stored using 16 bytes of memory. Consequently, the storage required on a classical computer to represent a pure

state of the system amounts to approximately 17 GB. Despite these computational challenges, many-body systems are worth studying, as they exhibit a rich variety of phenomena [26–29], driven by the correlations that emerge among their different degrees of freedom. Some of these correlations are purely classical, while others are inherently quantum in nature and will be the central focus of the following discussion.

Given a pure state $|\psi\rangle$, we define the *correlator*

$$C_{AB} = \langle O_A O_B \rangle - \langle O_A \rangle \langle O_B \rangle,$$

where O_A and O_B are operators acting on subsystems A and B respectively, and $\langle \cdot \rangle = \langle \psi | \cdot | \psi \rangle$ denotes the expectation value. If $C_{AB} = 0$ for all pairs of operators (O_A, O_B), then the two subsystems are uncorrelated. Conversely, if $C_{AB} \neq 0$ for at least one pair of operators, correlations exist between A and B; however, from this observation alone, we cannot determine whether these correlations are classical or quantum in nature. For this reason, we introduce a distinct definition of entanglement, which relies on the concept of separability. A state is said to be *separable* with respect to a bipartition A, B if and only if it can be written as

$$|\psi\rangle = |\psi_A\rangle \otimes |\psi_B\rangle \,.$$

It is straightforward to verify that, for a separable state, no correlations exist between the two subsystems. By contrast, a state is said to be *entangled* if it is not separable, $|\psi\rangle \neq |\psi_A\rangle \otimes |\psi_B\rangle$. In this situation, quantum correlations between A and B are necessarily present. A canonical example of an entangled state in a two-qubit system is the Bell state

$$|\psi\rangle = \frac{|01\rangle - |10\rangle}{\sqrt{2}} \,. \tag{2.1}$$

It is immediate to infer the separability of this state, but in general it can be quite challenging, especially for larger lattices. In such cases, it is convenient to introduce the Schmidt decomposition, which allows us to express the system state in a minimal form from which its separability can be immediately inferred. More precisely, it can be shown that there exist complete orthonormal bases $\{|\psi_i^A\rangle\}$ of $\mathcal{H}_A$ and $\{|\psi_i^B\rangle\}$ of $\mathcal{H}_B$ such that

$$|\psi\rangle = \sum_{i=1}^{r} \sqrt{p_i}\, |\psi_i^A\rangle\, |\psi_i^B\rangle \,, \tag{2.2}$$

where $r \leq D_A$ is the Schmidt rank and the coefficients $p_i \geq 0$ are real numbers satisfying $\sum_{i=1}^{r} p_i = 1$. Consequently, the state is entangled if more than one Schmidt coefficient is non-zero, or equivalently if the Schmidt rank $r > 1$, and separable otherwise. Although finding such a decomposition is still challenging and therefore rarely used in practical applications, its existence and formulation allow us to study further properties of entangled states.

2.2 Mixed states

Let us now consider a quantum system whose state is known to be one among a definite set $\{|\psi_i\rangle\}$, each occurring with probability $p_i \geq 0$, such that $\sum_i p_i = 1$. In this situation, the system cannot be described by a single state vector, but rather by a *density matrix*

$$\rho = \sum_i p_i\, |\psi_i\rangle\, \langle \psi_i| \,, \tag{2.3}$$

which represents a *statistical mixture* of all pure states in $\{|\psi_i\rangle\}$, encoding incomplete knowledge about the system. An extreme example is the maximally mixed state, described by the density matrix $\rho = \frac{1}{D}\mathbb{I}$, where $\mathbb{I}$ is the identity. This density matrix represents an equiprobable mixture of all pure states of the system and corresponds to complete uncertainty. On the other hand, if we know with probability

$p = 1$ that the system is in $|\psi\rangle$, which is the case of a pure state, then Eq. (2.3) reduces to the projector $\rho = |\psi\rangle\langle\psi|$.

Given a statistical mixture, the expectation value of an operator O is the probabilistic average

$$\langle O\rangle = \sum_i p_i \langle\psi_i| O |\psi_i\rangle .$$

It is straightforward to show that this definition implies

$$\langle O\rangle = \mathrm{Tr}(O\rho) = \sum_{l=1}^{D} \langle\psi_l| O\rho |\psi_l\rangle ,$$

where $\mathrm{Tr}(\cdot)$ denotes the trace and $\{|\psi_l\rangle\}$ is a complete orthonormal basis of the system. A density matrix is also characterized by the following properties: it is hermitian, $\rho^\dagger = \rho$; has unit trace, $\mathrm{Tr}(\rho) = 1$; and is positive semi-definite, $\langle\phi|\rho|\phi\rangle \geq 0 \quad \forall |\phi\rangle \in \mathcal{H}$. If ρ represents a pure state, then $\rho^2 = \rho$ and $\mathrm{Tr}(\rho^2) = 1$. These conditions are not satisfied in the case of a mixed state, where $\rho^2 \neq \rho$ and $\mathrm{Tr}(\rho^2) < 1$. For instance, if ρ represents a maximally mixed state, then $\mathrm{Tr}(\rho^2) = \frac{1}{D} < 1$. Indeed, $\mathrm{Tr}(\rho^2)$, called the *purity*, quantifies the degree to which a state is close to being pure.

Let us now generalize the concept of entanglement to mixed states, which is still defined through separability. In particular, a mixed state is said to be separable if it can be prepared using *local operations and classical communication* (LOCC). Imagine that the subsystems are in different laboratories: to prepare the system state with LOCC means that each laboratory can perform operations only on its own subsystem, and they can coordinate their actions solely through classical messages. In other words, we can write

$$\rho = \sum_i p_i \rho_i^A \otimes \rho_i^B .$$

In this case, some correlations between the subsystems can exist, but they are purely classical in nature. On the other hand, if a mixed state cannot be decomposed in this way, it is said to be entangled.

In the following, we will discuss entanglement measures, first focusing only on pure states and then generalizing the discussion to mixed states. In this context, it is useful to introduce the formalism of the *reduced density matrix*, which allows us to extract information about the states of subsystems A and B of a system prepared in a general state ρ. This is achieved for each subsystem by performing the partial trace of ρ over the degrees of freedom of the complementary subsystem. For example, the reduced density matrix of A is defined as

$$\rho_A = \mathrm{Tr}_B(\rho) = \sum_i \langle\psi_i^B|\rho|\psi_i^B\rangle ,$$

where $\{|\psi_i^B\rangle\}$ is a complete orthonormal basis for the Hilbert space of B. The reduced density matrix is itself a valid density matrix, since the partial trace preserves hermiticity, positivity, and normalization, and therefore satisfies all the defining properties. Moreover, it correctly encodes expectation values of operators acting solely on the subsystem. If O_A is an operator acting on subsystem A, then

$$\langle O_A\rangle = \mathrm{Tr}\left[(O_A \otimes \mathbb{I}_B)\,\rho\right] = \mathrm{Tr}\left(O_A\rho_A\right) .$$

2.3 Measures of entanglement

Consider the Bell state in Eq. (2.1), introduced as an example of an entangled pure state. The reduced density matrices of the two qubits are

$$\rho_A = \rho_B = \frac{1}{2}\left(|0\rangle\langle 0| + |1\rangle\langle 1|\right),$$

which represent mixed states. This means that observing one qubit, rather than the whole system, reveals that not all information is locally accessible and part of it is delocalized due to entanglement

between the two qubits. In this particular example, where the system state is maximally entangled and the qubits are in a maximally mixed state, no information is stored locally, and we have maximal ignorance about the state of each subsystem.

In general, if the global state is separable, the reduced density matrices correspond to pure states. If the global state is entangled, the reduced density matrices represent mixed states. This can be seen by considering the Schmidt decomposition in Eq. (2.2) when calculating the reduced density matrix:

$$\begin{aligned}\rho_A &= \mathrm{Tr}_B(|\psi\rangle\langle\psi|) \\ &= \sum_{i,j=1}^{r} \sqrt{p_i p_j}\, |\psi_i^A\rangle\langle\psi_j^A| \,\mathrm{Tr}(|\psi_i^B\rangle\langle\psi_j^B|) \\ &= \sum_{i=1}^{r} p_i\, |\psi_i^A\rangle\langle\psi_i^A|\,.\end{aligned}$$

If there is only one non-zero Schmidt coefficient $p_k \neq 0$, then $|\psi\rangle$ is separable and $\rho_A = |\psi_k^A\rangle\langle\psi_k^A|$ is a projector onto the pure state $|\psi_k^A\rangle$. On the other hand, if there is more than one non-zero Schmidt coefficient, then $|\psi\rangle$ is entangled and ρ_A represents a statistical mixture. From an informational perspective, this means that separable states imply maximal knowledge about the respective subsystems, while entangled states reflect a loss of local information due to non-local correlations across the parts of the system.

Therefore, we can exploit the fact that, in a bipartite system, the degree of mixedness of the subsystems' density matrices indicates how much information is not locally accessible, to quantify the entanglement in the system state. We first introduce the *von Neumann entropy* [30–33]

$$S(\rho) = -\mathrm{Tr}(\rho \log \rho)\,, \tag{2.4}$$

where the logarithm is taken in base two, without loss of generality. Since any density matrix is diagonalizable, the entropy simplifies to $S(\rho) = -\sum_{i=1}^{D} p_i \log p_i$. Several key properties follow from the definition in Eq. (2.4): $S(\rho) = 0$ if and only if ρ is a projector, i.e., represents a pure state; S is invariant under unitary transformations, $S(\rho) = S(U\rho U^\dagger)$; and $S(\rho) = N$ for a maximally mixed state of N qubits. Given a pure system's state $\rho = |\psi\rangle\langle\psi|$, the von Neumann entropy of either reduced density matrix, $S_A(|\psi\rangle) = S(\rho_A)$ and $S_B(|\psi\rangle) = S(\rho_B)$, can serve as a measure of entanglement. If $|\psi\rangle$ is separable with respect to a bipartition into subsystems A and B, then both ρ_A and ρ_B are pure, implying $S_A(|\psi\rangle) = S_B(|\psi\rangle) = 0$. In contrast, for an entangled pure state, the reduced density matrices are generally mixed and the von Neumann entropy is non-zero. In the maximally entangled case, the reduced states ρ_A and ρ_B are maximally mixed, and the von Neumann entropy reaches its maximum, $S_A(|\psi\rangle) = S_B(|\psi\rangle) = |A|$.

Unlike pure states, quantifying entanglement in mixed states is more challenging due to the coexistence of quantum and classical uncertainty, one arising from entanglement and the other from classical ignorance. As a result, it becomes essential to determine how much each contributes to the mixedness of the subsystems' states. Therefore, given the system state ρ and two local unitary operators, U_A and U_B, describing unitary transformations on the respective subsystems, the properties that an entanglement measure E must satisfy are: $E(\rho) = 0$ if and only if ρ represents a separable state; E is invariant under local unitary transformations, $E(\rho) = E\left((U_A \otimes U_B)\rho(U_A \otimes U_B)^\dagger\right)$; and entanglement cannot increase under LOCC or *sub-selection*, that is, the selection of a subset of measurement outcomes. In particular, the latter can be expressed as $E(\rho) \geq \sum_i p_i E(\rho_i)$, where ρ_i is obtained from ρ through a LOCC with probability p_i.

For mixed states, however, the von Neumann entropy of the reduced density matrix no longer reliably quantifies entanglement. This is caused by the fact that the decomposition of a mixed state into pure states $\{|\psi_i\rangle\}$ is not unique, causing the von Neumann entropy to depend on the chosen ensemble. Nevertheless, the entanglement entropy can be generalized to mixed states through the *entanglement of formation* [34]

$$E_F(\rho) = \min_{\{|\psi_i\rangle\}} \sum_i p_i S_A(|\psi_i\rangle)\,, \tag{2.5}$$

where the minimization is taken over all pure-state decompositions of ρ. Although conceptually straightforward, as it directly extends the von Neumann entropy definition of entanglement, this optimization problem can only be solved for small system sizes, due to the exponential growth of the Hilbert space dimension with the number of degrees of freedom.

An alternative entanglement measure is the *logarithmic negativity* [35]

$$\mathcal{N}_A(\rho) = \log \left\| \rho^{\mathrm{T}_A} \right\|_1 , \tag{2.6}$$

where $\| \cdot \|_1$ denotes the trace norm, defined as $\|O\|_1 = \mathrm{Tr}\left(\sqrt{O^\dagger O}\right) = \sum_i |\lambda_i|$, with O a generic operator and $\{\lambda_i\}$ its eigenvalues. This measure exploits a necessary condition, known as Peres-Horodecki criterion, which can be used to determine whether a mixed state is separable or entangled. If the system state ρ is separable, then its partial transpose, defined by $(\rho^{T_A})_{ab,a'b'} = \rho_{a'b,ab'}$, where the indices a, a' refer to subsystem A and b, b' to subsystem B, takes the form

$$\rho^{T_A} = \sum_i p_i \, (\rho_i^A)^T \otimes \rho_i^B \, .$$

which remains a valid density matrix. Consequently, all eigenvalues are non-negative and the trace norm is unity, giving $\mathcal{N}_A(\rho) = 0$. In contrast, if ρ is entangled, the partial transpose is no longer a valid density matrix, its eigenvalues can be negative, and the trace norm exceeds one, resulting in $\mathcal{N}_A(\rho) > 0$. The presence of even a single negative eigenvalue indicates that the system state is entangled. Therefore, logarithmic negativity measures entanglement by quantifying the extent to which the partially transposed state fails to be positive. Although evaluating this quantity requires calculating eigenvalues, which can be computationally demanding for large matrices, it is generally more efficient than the minimization required by the entanglement of formation.

Chapter 3

Open quantum many-body dynamics

In this chapter, we explore the time evolution of quantum many-body systems. We begin with closed systems, whose behavior is fully determined by the Schrödinger equation, and then extend the discussion to open systems, where coupling to an external environment introduces dissipation and decoherence, rendering the dynamics non-unitary. Throughout, we focus on time-independent Hamiltonians H that govern the system's evolution. Finally, we examine the symmetries of both closed and open systems, emphasizing their influence on the system's dynamics.

3.1 Time-evolution of many-body systems

We begin by analyzing closed systems, which are characterized by the absence of interactions and correlations with an external environment, ensuring that no information about the system's state is lost. Consequently, the system preserves the purity of its state over time. Specifically, if the system is initially prepared in a pure state $|\psi_0\rangle$, its time-evolution is governed by the Schrödinger equation

$$i\frac{\mathrm{d}}{\mathrm{d}t}|\psi(t)\rangle = H|\psi(t)\rangle \ , \tag{3.1}$$

where H denotes the system's Hamiltonian. For simplicity, we set $\hbar = 1$, which will be assumed implicitly in the following. The solution of Eq. (3.1) is $|\psi(t)\rangle = U(t)|\psi_0\rangle$, with $U(t) = e^{-iHt}$ the unitary time-evolution operator, which ensures that the norm of the state is preserved. If the initial state $|\psi_0\rangle$ is an eigenstate of the Hamiltonian, then $|\psi(t)\rangle = e^{-i\epsilon t}|\psi_0\rangle$, where ϵ is the corresponding energy eigenvalue. In this case, the system evolves only by acquiring a global phase, leaving all physical observables unchanged. Conversely, if the initial state is a superposition of Hamiltonian eigenstates, the system exhibits non-trivial dynamics, as relative phases develop between the components of the superposition.

The Schrödinger equation (3.1) can be extended to describe the time-evolution of a closed system, initially prepared in a mixed state ρ_0. Such a situation arises, for instance, when only partial knowledge of the system's state is available, although the uncertainty does not originate from correlations with an external environment. In this case, the dynamics of the system can still be expressed in terms of the unitary operator $U(t)$, which acts on the density matrix as $\rho(t) = U(t)\rho_0 U^\dagger(t)$. It can be shown that this relation is the solution of the von Neumann equation

$$i\frac{\mathrm{d}}{\mathrm{d}t}\rho(t) = [H, \rho(t)] \, , \tag{3.2}$$

which follows directly from the Schrödinger equation (3.1). The time-evolution described by Eq. (3.2) preserves both the trace and the purity of the density matrix.

The von Neumann equation (3.2) describes the unitary evolution of a mixed state but does not account for the possible loss of information to an external environment. For this reason, when dealing with an open system, it becomes necessary to extend this description. In particular, we introduce a set

of operators $\{L_k\}$, called *Lindblad operators*, which model the dissipative processes induced by the interaction of the system with its environment. These operators introduce a non-unitary contribution to the time-evolution, which is now described by the more general equation

$$\frac{\mathrm{d}}{\mathrm{d}t}\rho(t) = -i[H,\rho(t)] + \gamma \sum_k \left(L_k \rho(t) L_k^\dagger - \frac{1}{2}\{L_k^\dagger L_k, \rho(t)\} \right) , \tag{3.3}$$

known as the Gorini–Kossakowski–Sudarshan–Lindblad (GKSL) master equation [36], where $[\cdot,\cdot]$ and $\{\cdot,\cdot\}$ denote the commutator and anticommutator respectively, and γ is a parameter, which determines the strength of the interaction with the environment. It is important to note that this equation is derived under certain approximations. The first is the *Born approximation*, which assumes that the environment is much larger than the system and remains unaffected by the interaction. The second is the *Markov approximation*, which treats the environment as memoryless, ensuring that the evolution depends only on the current state and not on its history. It is also worth noting that for $\gamma = 0$ Eq. (3.3) reduces to the von Neumann equation (3.2), as expected.

To solve the master equation numerically it is convenient to cast it into a vectorized form [37], known as the *Liouvillian space representation*. In this formulation, the $D \times D$ density matrix ρ is reshaped into a D^2-dimensional vector, $\mathrm{vec}(\rho) = |\rho\rangle\rangle$, obtained by stacking its columns. Using the identity

$$|O_1 \rho O_2\rangle\rangle = (O_2^T \otimes O_1)\,|\rho\rangle\rangle \ ,$$

we can rewrite Eq. (3.3) as

$$\frac{\mathrm{d}}{\mathrm{d}t}\,|\rho(t)\rangle\rangle = \mathcal{L}\,|\rho(t)\rangle\rangle \ ,$$

where

$$\mathcal{L} = -i\left(\mathbb{I}\otimes H - H^T \otimes \mathbb{I}\right) + \gamma \sum_k \left(L_k \otimes L_k^* - \frac{1}{2}\mathbb{I}\otimes (L_k^\dagger L_k)^T - \frac{1}{2}(L_k^\dagger L_k)\otimes \mathbb{I} \right) ,$$

is the Liouvillian superoperator, which is a *completely positive trace-preserving* (CPTP) map. Consequently, given an initial state $|\rho_0\rangle\rangle$, the solution to the non-unitary time-evolution is

$$|\rho(t)\rangle\rangle = e^{\mathcal{L}t}\,|\rho_0\rangle\rangle \ . \tag{3.4}$$

It is important to note that the Liouvillian superoperator is generally not hermitian, $\mathcal{L}^\dagger \neq \mathcal{L}$, and therefore it is not necessarily diagonalizable, even though it always admits at least a block-diagonal decomposition. Its eigenvalues are in general complex, and there is always at least one eigenvalue equal to zero, referred to as the *fundamental eigenvalue*. The corresponding eigenvectors are the stationary states of the Liouvillian, satisfying $\mathcal{L}\,|\rho(t)\rangle\rangle = 0$. Such states remain invariant under the non-unitary evolution generated by $\mathcal{L}$ and represent equilibrium configurations of the system in the presence of environmental interactions.

3.2 Symmetries

In this section, we examine the role of symmetries in quantum mechanics, highlighting their effects on both the system's dynamics and its stationary states. In particular, we define a *symmetry* as a transformation of a physical system that leaves all observable predictions unchanged. In other words, the probabilities of measurement outcomes and the expectation values of operators remain invariant under such transformations. According to the Wigner theorem, any symmetry in quantum mechanics must be represented by either a unitary or an antiunitary transformation U.

Symmetries can be divided into two classes: *continuous symmetries*, described by continuously varying parameters $\boldsymbol{\epsilon}$, and *discrete symmetries*, involving only a finite set of transformations. Continuous symmetries are always realized by unitary operators and, via Noethers theorem, are associated with conserved quantities $\boldsymbol{G}$. These $\boldsymbol{G}$ are hermitian operators, known as *generators* of the symmetry,

and they commute with the Hamiltonian: $[G_j, H] = 0 \quad \forall G_j \in \boldsymbol{G}$. Thus a continuous symmetry transformation can be written as

$$U(\boldsymbol{\epsilon}) = e^{-i\boldsymbol{\epsilon}\cdot\boldsymbol{G}}\,.$$

Unitary transformations $U(\boldsymbol{\epsilon})$ on the Hilbert space form a *representation* of a Lie group $\mathcal{G}$ associated with the symmetry. At the same time, the corresponding generators $\boldsymbol{G}$, equipped with the commutator $[\cdot,\cdot]$, form the *Lie algebra* of $\mathcal{G}$, which describes the infinitesimal transformations within the symmetry. In particular, given the commutation relations of the generators

$$[G_a, G_b] = \sum_c f_{abc}\, G_c\,,$$

the f_{abc} coefficients are the *structure constants* of the Lie algebra.

Two important concepts regarding symmetries and their corresponding groups are *irreducible representations* and *symmetry sectors*. A representation is said to be irreducible if there is no non-trivial subspace of the Hilbert space that is invariant under the action of all group elements. Consequently, all states within the Hilbert space of an irreducible representation are connected by the symmetry transformations. On the other hand, since the Hamiltonian commutes with the generators of the symmetry, the Hilbert space decomposes into orthogonal subspaces, called sectors, which are invariant under the dynamics. Therefore a symmetry sector is a subspace of the Hilbert space determined by the eigenvalues of each generator of the symmetry. During time-evolution, the Hamiltonian may still mix states within the same sector, but it cannot connect states belonging to different sectors. Therefore, if the initial state lies in a given symmetry sector, the entire time-evolution remains confined to it.

Symmetries can also be classified as *Abelian* or *non-Abelian*. A symmetry is Abelian if all its generators commute, $[G_a, G_b] = 0 \quad \forall a, b$, thus corresponding to independent conserved quantities. In this case each irreducible representation is one dimensional, but inside the same symmetry sector there can be multiple irreducible representations that share the same eigenvalues of the symmetry generators. In contrast, a symmetry is non-Abelian if at least one structure constant is non-zero, $f_{abc} \neq 0$, so that some generators fail to commute. In this case irreducible representations can be multidimensional and organize into multiplets. As a consequence, the symmetry sectors can be intrinsically multidimensional, containing multiplets of states that share the same eigenvalues of the symmetry generators. It has recently been shown that, due to the fact that in non-Abelian symmetries the degeneracy is symmetry-enforced, stationary entangled states can emerge in the dynamics of the system [20, 38].

Motivated by this, in the next chapter we will investigate the role of symmetries in open-system dynamics. In this context, symmetries are more subtle and can be classified into two distinct classes: *strong symmetries* and *weak symmetries* [39]. A symmetry is called strong if both the Hamiltonian H and the Lindblad operators L_k are invariant under its transformations. In this case, if $\boldsymbol{G}$ denotes the generators of the symmetry, then the following commutation relations hold:

$$[H, G_j] = 0 \quad \text{and} \quad [L_k, G_j] = 0 \quad \forall G_j, L_k.$$

On the other hand, a weak symmetry requires only that the Liouvillian superoperator $\mathcal{L}$ is invariant, satisfying the weaker condition

$$[\mathcal{L}, \hat{G}_j] = 0 \quad \forall \hat{G}_j,$$

where

$$\hat{G}_j = G_j \otimes \mathbb{I} - \mathbb{I} \otimes G_j^T$$

is the superoperator corresponding to the symmetry generator G_j. Clearly, every strong symmetry is also a weak symmetry, but the converse is not true. The key distinction between these two cases lies in the possibility of associating conserved quantities with the symmetry in open-system dynamics. From the Master equation (3.3), one can derive an analogous equation for the expectation value of an operator. For the expectation value of a symmetry generator to be conserved, it must commute with both H and all L_k, which requires a strong symmetry. In contrast, weak symmetries, while constraining the structure of the Liouvillian, do not guarantee such conservations.

Chapter 4

The open 1D XXZ model

In this chapter, we study the dynamics of entanglement in a quantum lattice model in the presence of dissipation, using the tools introduced in Chapters 2 and 3. In particular, we focus on the spin-1/2 XXZ model in one spatial dimension, whose Hamiltonian is given by

$$H = J \sum_{j=1}^{N-1} \left(X_j X_{j+1} + Y_j Y_{j+1} + \Delta Z_j Z_{j+1} \right) , \tag{4.1}$$

where N is the number of lattice sites, J is the coupling constant, Δ is the anisotropy parameter, and

$$X = \begin{pmatrix} 0 & 1 \\ 1 & 0 \end{pmatrix} , \quad Y = \begin{pmatrix} 0 & -i \\ i & 0 \end{pmatrix} , \quad Z = \begin{pmatrix} 1 & 0 \\ 0 & -1 \end{pmatrix} ,$$

are the Pauli matrices. In Eq. (4.1) we use the shorthand notation $O_i O'_j = O_i \otimes O'_j$, which will be implied throughout the following discussion. From now on, we set $J = 1$, corresponding to antiferromagnetic interactions, meaning that neighboring spins tend to align in opposite directions.

Before proceeding to our analysis and simulations, we highlight the symmetries of the XXZ model, which play a central role in the dynamics of the systems under consideration. The first symmetry corresponds to invariance under rotations by an angle ϕ around the z-axis in spin space. This defines a representation of the U(1) Lie group, whose generator is the hermitian operator

$$Z_{\text{tot}} = \sum_{j=1}^{N} Z_j , \tag{4.2}$$

i.e., the *total magnetization* of the spin-chain. Indeed, one has $[H, Z_{\text{tot}}] = 0$, and the corresponding symmetry transformation is

$$U(\phi) = e^{-i\phi Z_{\text{tot}}} .$$

The U(1) symmetry is Abelian, and its sectors are labeled by M, the eigenvalue of the total magnetization operator Z_{tot}. For a spin-$\frac{1}{2}$ chain of length N, the dimension of the sector with magnetization M is given by $\binom{N}{N/2+M}$.

Of particular interest is the case $\Delta = 1$, which corresponds to the isotropic Heisenberg model. In this case, an additional symmetry emerges: the full spin-rotation invariance under arbitrary rotations by angles $\boldsymbol{\theta}$ in spin space. This defines a representation of the SU(2) Lie group, whose generators are the components of the total spin operator

$$\boldsymbol{S}_{\text{tot}} = (X_{\text{tot}},\ Y_{\text{tot}},\ Z_{\text{tot}})^T ,$$

where X_{tot} and Y_{tot} are defined analogously to Z_{tot} in Eq. (4.2). Indeed, for $\Delta = 1$ one has $[H, X_{\text{tot}}] = [H, Y_{\text{tot}}] = [H, Z_{\text{tot}}] = 0$, and the symmetry transformation can be expressed as

$$U(\boldsymbol{\theta}) = e^{-i\,\boldsymbol{\theta}\cdot\boldsymbol{S}_{\text{tot}}} .$$

The SU(2) symmetry is non-Abelian, and its sectors, composed of spin multiplets, are labeled by the total spin quantum numbers (S, M), where S is the eigenvalue of $\boldsymbol{S}^2_{\text{tot}} = X^2_{\text{tot}} + Y^2_{\text{tot}} + Z^2_{\text{tot}}$, and M is the eigenvalue of the total magnetization Z_{tot}.

4.1 Closed system dynamics

To analyze the impact of dissipation on entanglement dynamics, let us first consider a minimal example, which provides a convenient starting point, as it allows for analytical solutions to verify our numerical framework. For instance, consider a closed system composed of two qubits, in this case the Hamiltonian from Eq. (4.1) reads

$$H = X_1X_2 + Y_1Y_2 + \Delta Z_1Z_2\,, \tag{4.3}$$

where we set $J = 1$. By diagonalizing Eq. (4.3), we obtain the eigenvalues λ_i and their corresponding degeneracies d_i,

$$\begin{aligned} \lambda_1 &= \Delta && \text{with } d_1 = 2\,,\\ \lambda_2 &= -\Delta + 2 && \text{with } d_2 = 1\,,\\ \lambda_3 &= -\Delta - 2 && \text{with } d_3 = 1\,, \end{aligned}$$

together with the eigenvectors $|v_i\rangle$,

$$|v_1\rangle = \begin{pmatrix}1\\0\\0\\0\end{pmatrix}, \quad |v_2\rangle = \begin{pmatrix}0\\0\\0\\1\end{pmatrix}, \quad |v_3\rangle = \frac{1}{\sqrt{2}}\begin{pmatrix}0\\1\\1\\0\end{pmatrix}, \quad |v_4\rangle = \frac{1}{\sqrt{2}}\begin{pmatrix}0\\1\\-1\\0\end{pmatrix}.$$

Let us now consider the initial state $|\psi_0\rangle = |01\rangle$, a pure, separable state with the spins pointing in opposite directions, Fig. 4.1 (a). Since $|\psi_0\rangle$ is not an eigenstate of H, its time-evolution is non-trivial and to compute it, it is convenient to express $|\psi_0\rangle$ in the eigenbasis of H:

$$|\psi_0\rangle = \frac{1}{\sqrt{2}}(|v_3\rangle + |v_4\rangle)\,.$$

Using this decomposition, the time-evolved state can be written as

$$|\psi(t)\rangle = e^{i\Delta t}\left[\cos(2t)\,|01\rangle - i\sin(2t)\,|10\rangle\right]\,.$$

The global phase factor $e^{i\Delta t}$ is physically irrelevant and can be discarded, so that the dynamics is fully captured by the relative phases between $|01\rangle$ and $|10\rangle$. The density matrix of the system then reads

$$\rho(t) = |\psi(t)\rangle\langle\psi(t)| = \begin{pmatrix}0 & 0 & 0 & 0\\ 0 & \cos^2(2t) & \frac{i}{2}\sin(4t) & 0\\ 0 & -\frac{i}{2}\sin(4t) & \sin^2(2t) & 0\\ 0 & 0 & 0 & 0\end{pmatrix}.$$

To study the entanglement, we focus on the reduced state of the first qubit, denoted as A (see Chapter. 2). By tracing out qubit B, we obtain

$$\rho_A(t) = \text{Tr}_B(\rho(t)) = \begin{pmatrix}\cos^2(2t) & 0\\ 0 & \sin^2(2t)\end{pmatrix}.$$

This expression allows us to track the purity of the reduced state over time. Specifically, for $t = k\frac{\pi}{4}$ with $k \in \mathbb{N}$, ρ_A becomes a projector onto a pure state, while for $t = \frac{\pi}{8} + k\frac{\pi}{4}$ both eigenvalues are equal to $\frac{1}{2}$, corresponding to a maximally mixed state. Hence, the entanglement oscillates between zero, when the global state is separable, and one, when it is maximally entangled. Defining $p = \cos^2(2t)$ as

the probability of measuring the first qubit in the state $|0\rangle$, and $1-p = \sin^2(2t)$ as the probability of measuring it in $|1\rangle$, the von Neumann entropy of qubit A is

$$S_A = -p\log(p) - (1-p)\log(1-p)\,,$$

which oscillates periodically between 0 and 1, as expected. Since the global evolution is unitary, the total state remains pure at all times, and the entanglement does not decay but rather exhibits persistent oscillations. Numerical simulations of the system, together with the computation of the von Neumann entropy, confirm excellent agreement with the analytical results, as shown in Fig. 4.1 (a), which displays the entropy as a function of time. All details regarding the numerical implementations can be found in Appendix A.

We now turn to the many-body case, where richer and more complex phenomena emerge. The dimension of the Hilbert space $\mathcal{H}$ grows exponentially with the number of lattice sites, making analytical solutions unfeasible. Therefore, from now on, we present only numerical simulations, of which we first outline the details and then present the results obtained. We consider an initially separable state $|\psi_0\rangle = |0101\ldots\rangle$, known as Néel state, in which neighboring qubits point in opposite directions, see Fig. 4.1 (b). After constructing the XXZ Hamiltonian from Eq. (4.1) for N qubits, see Code A.1, we numerically compute its eigenvalues and eigenvectors using the `eigh` routine from the `scipy.linalg` package [40]. Due to the increasing memory demands of larger systems, and the fact that larger Hamiltonians from Eq. 4.1 tend to contain an increasing number of zero entries, we choose to work with sparse matrices and employ the `scipy.sparse` package [40]. The procedure then follows the same steps as in the two-qubit case, with the main difference that we now evaluate the von Neumann entropy for each spatially connected bipartition of the system. In this context, a more efficient approach is required for the extraction of the reduced density matrix. Building the projector explicitly is computationally demanding and, moreover, unnecessary, since all information is already encoded in the state vector $|\psi\rangle$. Let us recall that D denotes the dimension of the full system, D_A the dimension of the first subsystem, and D_B that of the second subsystem. By reshaping $|\psi\rangle$ into a $D_A \times D_B$ matrix C, we can then compute the reduced density matrix as $\rho_A = CC^\dagger$, in a significantly more efficient way, see Code A.2.

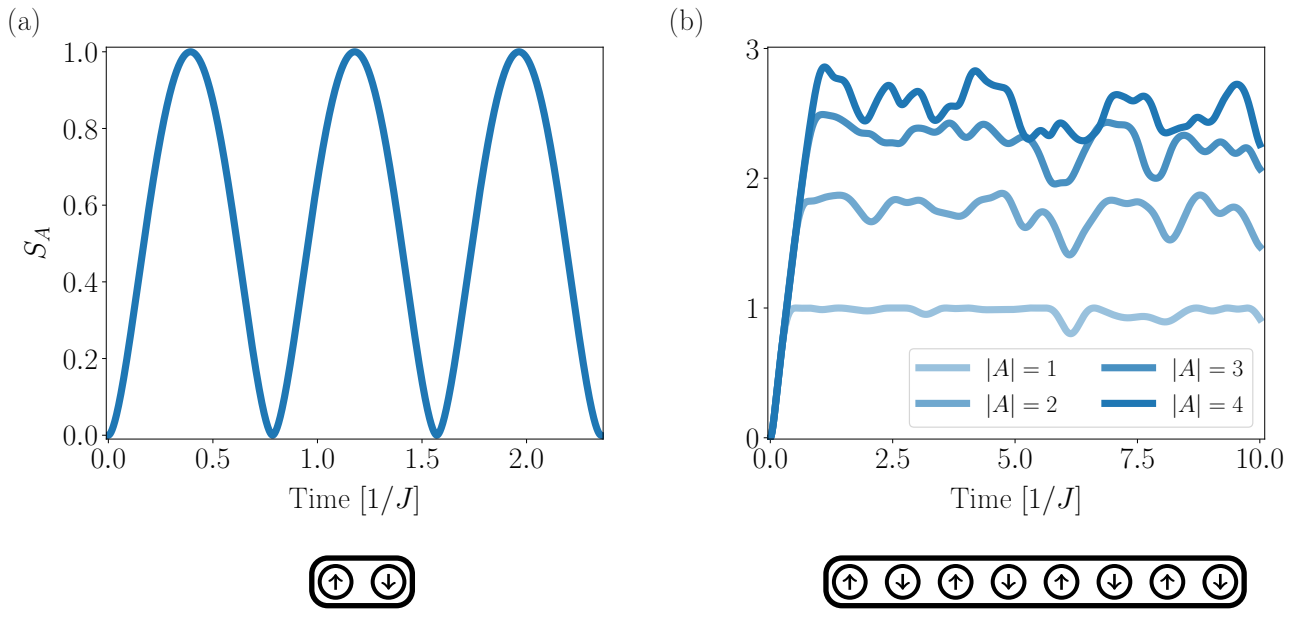

Figure 4.1: (a) Dynamics of von Neumann entropy (2.4) following a quench from the initial state $|\psi_0\rangle = |01\rangle$ under the Hamiltonian (4.3) for a system of $N = 2$ lattice sites. (b) Dynamics of von Neumann entropy (2.4) for each spatially connected bipartition following a quench from the initial state $|\psi_0\rangle = |01010101\rangle$ under the Hamiltonian (4.1) for a system of $N = 8$ lattice sites. The schematics below represent the respective initial states.

We show in Fig. 4.1 (b) the dynamics of the von Neumann entropy for different bipartitions, considering

a system of 8 qubits. Initially, the entropy of each bipartition is zero, consistent with the separability of the initial state. It then increases linearly with time, displaying the same slope across all bipartitions, before saturating at a value proportional to the size of the smaller subsystem, as expected. Finite-size effects give rise to small fluctuations, which decrease with increasing system size. Overall, the behavior of the von Neumann entropy over time shows that the interaction described by the XXZ Hamiltonian generates correlations among different parts of the system, driving it toward an highly entangled state. Each subsystem effectively equilibrates with the rest of the lattice, and most of the local information about its initial configuration is lost due to the emergence of non-local correlations.

4.2 Open system dynamics

We now extend the discussion of the XXZ model to open systems, analyzing how dissipative processes and symmetries affect the entanglement dynamics. In particular, we present the main result of our study: the emergence of entangled stationary states, enabled by non-Abelian strong symmetries.

We first model the interaction between the system and its environment using the Lindblad operators $L_j = Z_j$, which act as the Z operator on the j-th qubit and as the identity on all others. This choice corresponds to pure dephasing noise, which does not affect the populations, i.e. the diagonal elements of the density matrix, but gradually suppresses the off-diagonal elements, namely the coherences, over time. In other words, it destroys superpositions while leaving the probabilities of measuring $|0\rangle$ or $|1\rangle$ unchanged. Physically, this describes the coupling of each qubit to an environment that "measures" it in the computational basis, for instance due to fluctuations of an external magnetic field along the z-axis.

After computing the Liouvillian superoperator for $\Delta = 1$ and $\gamma = 0.05\,J$, see Code A.3, we evaluate the time-evolution of an 8-qubit system initially prepared in the Néel state. The dynamics is obtained by vectorizing the density matrix and numerically solving Eq. (3.4) using the routine `expm_multiply` from the `scipy.sparse.linalg` package [40]. In this case, we compute both the von Neumann entropy Eq. (2.4) and the logarithmic negativity Eq. (2.6), considering a bipartition of the system into two halves, see Code A.4. The dynamics of these quantities is shown in Fig. 4.2, light lines. Initially, both the logarithmic negativity and the von Neumann entropy grow linearly, as in the closed-system case. However, while the logarithmic negativity reaches a maximum value and then rapidly decays toward zero, the von Neumann entropy continues to increase and approaches an asymptotic value. As discussed in Chapter 2, the logarithmic negativity quantifies the system's entanglement, whereas the von Neumann entropy also includes correlations with the environment. Here, subsystem A equilibrates not only due to interactions with subsystem B but also due to interactions with the environment. At the same time, dissipation generates correlations between the system and its surroundings, so that after sufficient time all local information flows outward. This leads the entropy to increase toward its asymptotic value, while entanglement decays. Thus, at long times, the loss of local information is not caused by entanglement between subsystems but rather by correlations with the environment.

We now compare these results with those obtained choosing the Lindblad operators $L_j = Y_j$. In the computational basis, this type of noise affects both populations and coherences: it suppresses the off-diagonal elements, thereby destroying superpositions, and also induces transitions between $|0\rangle$ and $|1\rangle$. Physically, this models the coupling of each qubit to an environment that effectively "measures" it along the y-axis, for instance due to fluctuations in that direction, causing both dephasing and bit flips.

By simulating the system with the same parameters, we obtain the results shown in Fig. 4.2 dark lines. The behavior of the logarithmic negativity over time is qualitatively similar to that observed in the previous simulation: it exhibits an initial linear growth, followed by a peak, and then a decay toward zero at long times. The key difference lies in the maximum entropy reached by subsystem A. While in the simulation with $L_j = Y_j$ the entropy saturates to the maximum value expected from the discussion in Chapter 2, namely $|A| = 4$, in the simulation with $L_j = Z_j$ the saturation value is lower, along with a slower decay of the logarithmic negativity. This difference arises from the system's

symmetries. In the simulation with $L_j = Y_j$, the initial state is not an eigenstate of Y_{tot}, now the generator of the U(1) strong symmetry, and consequently the stationary state can explore the entire Hilbert space $\mathcal{H}$, allowing the system to lose all information about its initial configuration. By contrast, in the simulation with $L_j = Z_j$, the system is initialized in a state entirely contained within a sector of fixed total magnetization, which remains conserved over time. In this scenario, the expected maximum entropy for an N-qubit system, with respect to a bipartition into two halves, is

$$S_A^{(M)}(N) = -\sum_{M=0}^{N/2} \binom{N/2}{M} \frac{\binom{N/2}{M}}{\binom{N}{N/2}} \log \frac{\binom{N/2}{M}}{\binom{N}{N/2}} .$$

For $N = 8$, it assumes the value $S_A^{(M)}(8) \approx 3.885$, in perfect agreement with our numerical result, as shown in Fig. 4.2 (a).

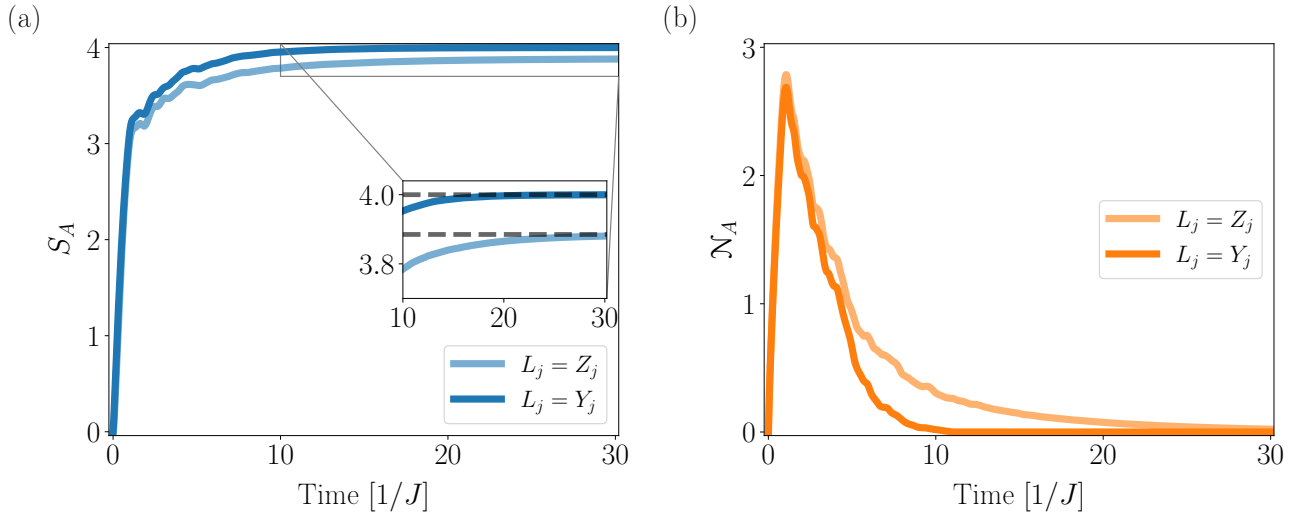

Figure 4.2: Dynamics of (a) von Neumann entropy (2.4) and (b) logarithmic negativity (2.6) following a quench from the initial state $|\psi_0\rangle = |01010101\rangle$ under the Hamiltonian (4.1) and Lindblad operators $L_j = Z_j$ (light lines), $L_j = Y_j$ (dark lines), for a system of $N = 8$ lattice sites.

Although some information about the initial state is preserved, such as the total magnetization, the logarithmic negativity still vanishes at long times, indicating relaxation to a separable stationary state. However, as discussed in Sec. 3.2, if the dynamics is confined to a sector of a strong non-Abelian symmetry, such as SU(2), the system is expected to relax to an entangled stationary state. Consequently, it is necessary to model the coupling between system and its environment using Lindblad operators that commute with the generators of the SU(2) symmetry. To this end, we choose them analogously to the Hamiltonian itself, yielding

$$L_j = X_j X_{j+1} + Y_j Y_{j+1} + Z_j Z_{j+1} . \tag{4.4}$$

If the initial state lies within a sector whose degeneracy is enforced by the non-Abelian symmetry, and the eigenvalues of the generators are preserved thanks to the strong symmetry, then the system remains confined to that sector. We first choose as the initial state of the N-qubit system the tensor product of $N/2$ Bell states, Eq. (2.1), where two neighboring qubits form a Bell pair, see Fig. 4.3 (a). The initial state is thus expressed as

$$|\psi_0\rangle = \bigotimes_{j=1}^{N/2} \frac{1}{\sqrt{2}} (|01\rangle - |10\rangle)_{2j-1,2j} \tag{4.5}$$

This state is separable with respect to a bipartition into two halves; however, it already contains entanglement arising from the construction of the Bell pairs. Moreover, such a state is fully contained within a symmetry sector of SU(2). It is straightforward to verify that $|\psi_0\rangle$ is an eigenstate of both

Z_{tot} with eigenvalue zero and S^2_{tot} with eigenvalue zero. Evolving this state and computing both the von Neumann entropy Eq. (2.4) and the logarithmic negativity Eq. (2.6) we obtain the results displayed in Fig. 4.3 (a). As expected, the initial state exhibits no entanglement. The logarithmic negativity increases, as in the previous simulations, and then reaches a maximum. Crucially, in this case the entanglement does not fully decay: the system relaxes into an entangled stationary state despite the presence of dissipation. At the same time, the von Neumann entropy saturates but does not reach its maximum value, since the dynamics of the system is now confined within both a magnetization sector and a total-spin sector.

We next consider a similar initialization, but this time the Bell pairs are formed between mirror-symmetric qubits, for instance, the first with the last, the second with the penultimate, and so on, see Fig. 4.3 (b). The initial state is thus expressed as

$$|\psi_0\rangle = \bigotimes_{j=1}^{N/2} \frac{1}{\sqrt{2}} \left(|01\rangle - |10\rangle\right)_{j,N-j+1} \tag{4.6}$$

Simulating the system under the same parameters yields the results shown in Fig. 4.3 (b). In this case, the initial state is entangled with respect to a bipartition into two halves, as indicated by the logarithmic negativity being maximal at $t = 0$. The subsequent dissipation processes reduce the entanglement until it stabilizes at a non-zero value. Thus, also in this case, the system evolves into a stationary entangled state. Remarkably, the stationary states reached in both simulations coincide, indicating that their respective initial states belong to the same SU(2) symmetry sector.

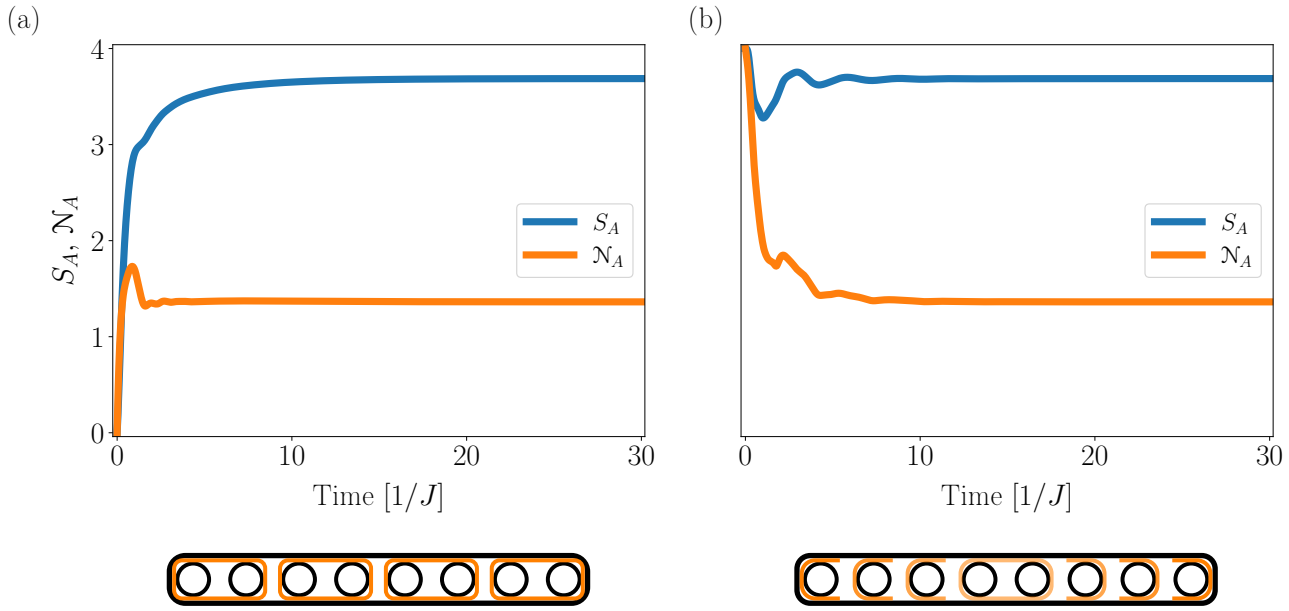

Figure 4.3: Dynamics of von Neumann entropy (2.4) and logarithmic negativity (2.6) following a quench under the Hamiltonian (4.1) and Lindblad operators (4.4) for a system of $N = 8$ lattice sites. (a) Initial state from Eq. (4.5). (b) Initial state from Eq. (4.6). The schematics below represent the respective initial states.

Although these results are promising, as they show at least a partial preservation of entanglement over long times, it is necessary to highlight some potential limitations of this approach. First, the simulations assume perfect engineering of both the system and its environment. For example, if the qubits composing the system couple to an environment not only through the Lindblad operators in Eq. (4.4), but also via $L_j = Y_j$, then the SU(2) symmetry of the system is no longer strong. This occurs because the symmetry generators $\boldsymbol{S}_{tot}$ do not commute with $L_j = Y_j$. In such a case, the system dynamics is no longer restricted to a symmetry sector of a non-Abelian symmetry and entanglement is free to decay toward zero. Simulating the system with $\Delta = 1$ and $\gamma = 0.05\,J$, and choosing as initial state the one in Eq. (4.5), we obtain the results in Fig. 4.4. The von Neumann entropy increases until it saturates at an asymptotic value lower than the theoretical prediction in Chapter 2, namely

$|A| = 4$. This reduction is again due to the presence of a U(1) strong symmetry, which constrains the dynamics to the symmetry sector containing the initial state. In this case, however, the relevant symmetry corresponds to rotations of arbitrary angle ϕ around the y-axis in spin space, generated by $Y_{tot} = \sum_j Y_j$, which commutes with both H and L_k. The state in Eq. (4.5) is, indeed, an eigenstate of Y_{tot}, thus satisfying the conditions for the observed results. The logarithmic negativity instead shows an initial growth, quickly suppressed by the dissipative processes. After reaching a peak, lower than the one obtained with only the Lindblad operators of Eq. (4.4), see Fig. 4.3 (b), the logarithmic negativity decays toward zero. In summary, dissipative processes other than those specifically engineered to preserve entanglement can break the SU(2) strong symmetry, resulting in vanishing entanglement.

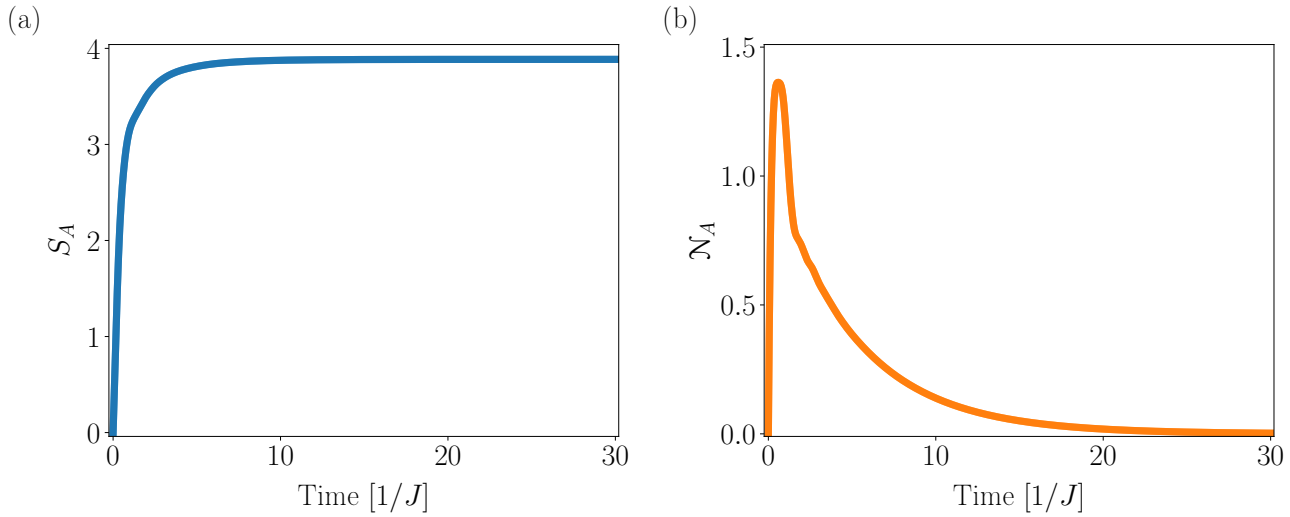

Figure 4.4: Dynamics of (a) von Neumann entropy (2.4) and (b) logarithmic negativity (2.6) following a quench with initial state from Eq. (4.5) under the Hamiltonian (4.1) and Lindblad operators from Eq. (4.4) and $L_j = Y_j$ for a system of $N = 8$ lattice sites.

It is also worth noting that retaining even a fraction of the total entanglement of an N-qubits system initialized in the state of Eq. (4.5) requires the prior construction of $N_{\text{Bell}} = N/2$ Bell pairs. This means that the initial state contains more entanglement than the stationary state. Consequently, following this procedure leads us to lose entanglement over time, rather than gaining it. To show how this phenomenon scales with the dimensions of the system, we plot in Fig. 4.5 (a) the logarithmic negativity of the stationary state $\mathcal{N}_A^{\text{stat}}$ against the number of sites N of the system. We observe that the entanglement grows linearly with N, once the point at $N = 4$, which ca be seen to be an outlier, is excluded. For $N = 2$, the system is in the singlet state of Eq. (2.1), an eigenstate of both the Hamiltonian and the Lindblad operators. Thus, both preserve the state and its entanglement, which remains maximal, i.e. one, over time. For $N = 4$, the local Lindblad operators L_1 and L_3 act on the first and second pair respectively, leaving them unchanged, while L_2 acts non-trivially between sites 2 and 3, generating entanglement across the bipartition. Due to U(1) and SU(2) constraints, the only possible stationary state for the pair 2–3 is the singlet state, again giving an entanglement of one with respect to the bipartition into two halves. For $N \geq 6$, several Lindblad operators act across different Bell pairs, and the Liouvillian mixes a larger subspace of states. The stationary state then lies in a bigger symmetry sector. With more degrees of freedom, the system redistributes entanglement more freely, scaling linearly with N. The anomalous behavior at $N = 4$ is thus attributed to finite-size effects absent in larger systems. However, even though residual entanglement scales linearly with the number of qubits, it must be compared with the initial entanglement provided by N_{Bell} Bell pairs. Since each Bell pair contributes one unit of entanglement, the total initial entanglement equals N_{Bell}. In Fig. 4.5 (b), we plot the ratio between stationary and initial entanglement against the number of sites N. The ratio decreases toward zero as N increases, meaning that larger systems require the creation of more entanglement to preserve an ever smaller fraction of it.

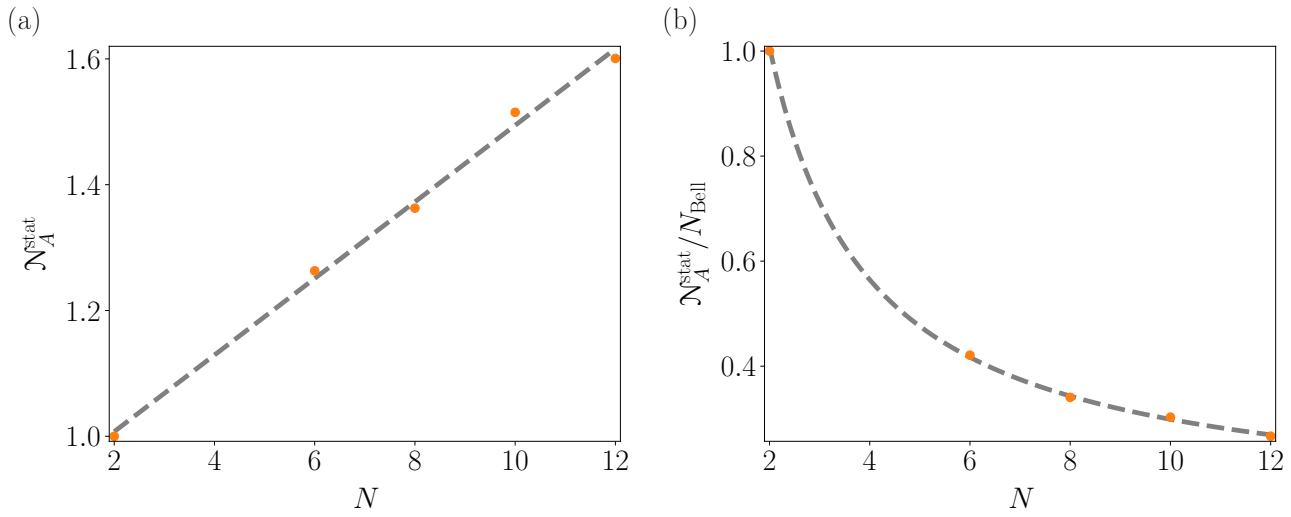

Figure 4.5: (a) Logarithmic negativity of the stationary state $\mathcal{N}_A^{\text{stat}}$, following a quench with initial state from Eq. (4.5) under the Hamiltonian (4.1) and Lindblad operators (4.4), as a function of the number of sites. (b) Ratio between $\mathcal{N}_A^{\text{stat}}$ and the number of Bell pairs N_{Bell}, as a function of the number of sites.

Chapter 5

Conclusion

In this work, we discussed the main theoretical framework required to study the dynamics of open quantum many-body systems and their bipartite entanglement. In particular, we first introduced an informational perspective on entanglement, reviewing the most relevant measures: the von Neumann entropy (2.4), the entanglement of formation (2.5), and the logarithmic negativity (2.6). We then described how to model dissipative processes via Lindblad operators and how to compute the time-evolution of open quantum systems through the Gorini–Kossakowski–Sudarshan–Lindblad (GKSL) master equation (3.3). Moreover, we investigated the role of symmetries in quantum mechanics and showed how they can shape the dynamics of open systems, allowing them to relax into non-trivial stationary states. Most notably, we highlighted a recent result by Pollmann et al. [20,38], demonstrating that in the presence of a strong non-Abelian symmetry such as SU(2), entanglement can survive in the stationary state despite dissipation. Motivated by this, we studied entanglement dynamics following a quantum quench under the XXZ Hamiltonian, through numerical simulations. First we considered closed systems and we studied the dynamics of the von Neumann entropy for different spatially connected bipartitions. Finally, we introduced dissipative processes, choosing different couplings between system and environment.

Our analysis led to the following conclusions: (i) In the closed quantum many-body systems we considered, each subsystem effectively equilibrates with the rest of the system, and local information is lost due to the build-up of non-local correlations, namely entanglement. (ii) In the open quantum many-body systems we considered, subsystems also equilibrate with the environment. Without a strong symmetry constraining the dynamics to a specific symmetry sector of the Hilbert space, all information about the initial state is lost, as it flows toward the environment, and entanglement vanishes. (iii) A strong Abelian symmetry, such as U(1), does not prevent this behavior. Entanglement still decays, though the stationary state retains some information about the initial configuration, as for example the total magnetization. (iv) A strong non-Abelian symmetry, such as SU(2), enables the systems we considered to relax into an entangled stationary state, despite dissipative processes.

While these results represent an important step toward understanding and engineering open quantum systems whose entanglement is robust against dissipation, they come with notable limitations: (i) The construction of the environment is fragile; small unwanted couplings can break the strong non-Abelian symmetries, resulting in vanishing entanglement over time. (ii) We obtained an entangled stationary state only for initial states which possess even more entanglement, resulting in a net loss of quantum correlations over time. (iii) Although the entanglement of the stationary state scales linearly with system size, it represents an ever smaller fraction of the initial entanglement. Thus, in practical implementations, the benefits of preserving some entanglement are outweighed by the difficulty of preparing strongly entangled initial states.

These findings suggest several promising directions for future research. Can entangled stationary states emerge from the dynamics of an open system initially prepared in a separable state? Can the requirement of strong non-Abelian symmetries be relaxed? Can we obtain similar behaviors with

the presence of only weak symmetries and the resulting structural constraints in the Liouvillian? Is it possible to engineer conditions under which the system relaxes into a pure, rather than mixed, stationary state, preserving also the superpositions? Addressing these questions could open the door to new ways of creating and protecting entanglement in open quantum many-body systems. Such advances may not only revolutionize quantum computing but also unlock new tools for probing the fundamental principles of the physical world.

Appendix A

Code for numerical simulations

Here we report the code for the numerical simulations referenced throughout this thesis. The complete implementation can be found in our GitHub repository.

```
h = csr_matrix((2**sites, 2**sites), dtype=complex)
for site in range(0, sites - 1):
    i1 = identity(2**site, format='csr', dtype=complex)
    i2 = identity(2 ** (sites - site - 2), format='csr', dtype=complex)
    h += (kron(kron(kron(i1, X), X), i2) +
          kron(kron(kron(i1, Y), Y), i2) +
          delta * kron(kron(kron(i1, Z), Z), i2))
```

Code A.1: Code used for the computation of the XXZ Hamiltonian for differene value of Δ and number of lattice sites N.

```
# Compute time-evolution operator
d_exp = diags(np.exp(-1j * evals * dt), 0, format='csr')
U = evecs.dot(d_exp).dot(evecs.getH())
# Track entropy over time
s_matrix = np.zeros((int(sites / 2), t_steps))
for _ in range(t_steps):
    for div in range(1, int(sites / 2) + 1):
        d1, d2 = 2 ** div, 2 ** (sites - div)
        # Reduced density matrix
        C = psi0.toarray().reshape(d1, d2)
        rho1 = C @ C.conj().T
        # Von Neumann entropy
        s_vals = np.linalg.eigvalsh(rho1)
        s_vals = s_vals[s_vals > 1e-12]
        s_matrix[div - 1][t] = -np.sum(s_vals * np.log2(s_vals))
    # Evolve state
    psi0 = U.dot(psi0)
```

Code A.2: Code used for simulating the time-evolution of a closed system and computing the von Neumann entropy for each spatially connected bipartition.

```
l_sup_op = -1j * (kron(i, h) - kron(h.T, i))
not_unitary = csr_matrix((2**(2 * sites), 2**(2 * sites)), dtype=complex)
for j, l_op in enumerate(l_ops):
    not_unitary += kron(l_op, l_op.conjugate())
    not_unitary -= 0.5 * (kron(i, (l_op.getH().dot(l_op)).T) +
                          kron(l_op.getH().dot(l_op), i))
l_sup_op += gamma * not_unitary
```

Code A.3: Code used for the computation of the Liouvillian superoperator, given a set of Lindblad operators L_k, for different values of γ.

```
for t in range(t_steps):
    ...
    # -- Von Neumann entropy --
    entropy = -np.sum(s_vals * np.log2(s_vals))
    # -- Logarithmic negativity --
    # Partial transpose on subsystem B
    rho_pt = np.transpose(rho, axes=(0, 3, 2, 1))
    rho_pt = rho_pt.reshape((2 ** sites, 2 ** sites), order='F')
    #
    ln_arr.append(np.log2(np.linalg.norm(rho_pt, ord='nuc')))
    # -- Time evolution --
    rho = expm_multiply(L_dt, rho)
```

Code A.4: Code used for simulating the time-evolution of an open system and computing the logarithmic negativity for a bipartition into two halves.

Bibliography

[1] Albert Einstein, Boris Podolsky, and Nathan Rosen. Can quantum-mechanical description of physical reality be considered complete? *Physical Review*, 47(10):777–780, 1935.

[2] Erwin Schrödinger. Discussion of probability relations between separated systems. *Mathematica Slovaca*, 5:136–138, 1935.

[3] David Bohm. A suggested interpretation of the quantum theory in terms of "hidden" variables. *Physical Review*, 85(2):166–179, 1952.

[4] John S. Bell. On the einstein podolsky rosen paradox. *Physics Physique* , 1(3):195–200, 1964.

[5] John F. Clauser, Michael A. Horne, Abner Shimony, and Richard A. Holt. Proposed experiment to test local hidden-variable theories. *Physical Review Letters*, 23(15):880–884, 1969.

[6] S. J. Freedman and J. F. Clauser. Experimental test of local hidden-variable theories. *Physical Review Letters*, 28(14):938–941, 1972.

[7] Alain Aspect, Jean Dalibard, and Gérard Roger. Experimental test of bell's inequalities using time-varying analyzers. *Physical Review Letters*, 49(25):1804–1807, 1982.

[8] Alain Aspect, Philippe Grangier, and Gérard Roger. Experimental realization of einstein–podolsky–rosen–bohm gedankenexperiment: A new violation of bell's inequalities. *Physical Review Letters*, 49(2):91–94, 1982.

[9] M. A. Rowe, D. Kielpinski, V. Meyer, C. A. Sackett, W. M. Itano, C. Monroe, and D. J. Wineland. Experimental violation of a bell's inequality with efficient detection. *Nature*, 409:791–794, 2001.

[10] B. Hensen, H. Bernien, A. E. Dréau, A. Reiserer, N. Kalb, M. S. Blok, L. T. Schouten, J. K. W. van Dijk, M. Markham, D. J. Twitchen, L. Childress, and R. Hanson. Loophole-free bell inequality violation using electron spins separated by 1.3 kilometers. *Nature*, 526:682–686, 2015.

[11] M. Giustina, A. Mech, S. N. Atalaya, J. Kofler, T. Jennewein, T. Lita, S. W. Nam, R. Ursin, and A. Zeilinger. Significant-loophole-free test of bell's theorem with entangled photons. *Physical Review Letters*, 115(25):250401, 2015.

[12] R. Horodecki, P. Horodecki, M. Horodecki, and K. Horodecki. *Rev. Mod. Phys.*, 81:865, 2009.

[13] Artur K. Ekert. Quantum cryptography based on bell's theorem. *Physical Review Letters*, 67(6):661–663, 1991.

[14] Charles H. Bennett and Stephen J. Wiesner. Communication via one- and two-particle operators on einstein–podolsky–rosen states. *Physical Review Letters*, 69(20):2881–2884, 1992.

[15] Charles H. Bennett, Gilles Brassard, Claude Crépeau, Richard Jozsa, Asher Peres, and William K. Wootters. Teleporting an unknown quantum state via dual classical and einstein–podolsky–rosen channels. *Physical Review Letters*, 70(13):1895–1899, 1993.

[16] David Deutsch. Quantum theory, the church–turing principle and the universal quantum computer. *Proceedings of the Royal Society of London. Series A, Mathematical and Physical Sciences*, 400(1818):97–117, 1985.

[17] Richard P. Feynman. Simulating physics with computers. *International Journal of Theoretical Physics*, 21(6-7):467–488, 1982.

[18] Peter W. Shor. Scheme for reducing decoherence in quantum computer memory. *Physical Review A*, 52(4):R2493–R2496, 1995.

[19] Andrew M. Steane. Error correcting codes in quantum theory. *Physical Review Letters*, 77(5):793–797, 1996.

[20] Y. Li, F. Pollmann, N. Read, and P. Sala. *arXiv:2406.08567*.

[21] S. Ebadi, T. T. Wang, H. Levine, A. Keesling, G. Semeghini, A. Omran, D. Bluvstein, R. Samajdar, H. Pichler, W. W. Ho, S. Choi, S. Sachdev, M. Greiner, Vuletić, and M. D. Lukin. *Nature*, 595:227–232, 2021.

[22] C. Noel, P. Niroula, D. Zhu, A. Risinger, L. Egan, D. Biswas, M. Cetina, A. V. Gorshkov, M. J. Gullans, D. A. Huse, and C. Monroe. *Nature Physics*, 18:760–764, 2022.

[23] N. Nishad, A. Keselman, T. Lahaye, A. Browaeys, and S. Tsesses. *Phys. Rev. A*, 108:053318, 2023.

[24] M. K. Joshi, C. Kokail, R. van Bijnen, F. Kranzl, T. V. Zache, R. Blatt, C. F. Roos, and P. Zoller. *Nature*, 624:539–544, 2023.

[25] D. Adler, D. Wei, M. Will, K. Srakaew, S. Agrawal, P. Weckesser, R. Moessner, F. Pollmann, I. Bloch, and J. Zeiher. *Nature*, 636:80–85, 2024.

[26] A. J. Daley. Quantum many-body systems out of equilibrium. *arXiv preprint arXiv:1408.5148*, 2014.

[27] J. Alvarez et al. Revealing emergent many-body phenomena by analyzing large-scale space-time records of monitored quantum systems. *arXiv preprint arXiv:2507.00944*, 2025.

[28] Anonymous. Emergent and topological phenomena in many-body systems. PhD Dissertation, Harvard University, 2025.

[29] MDPI Entropy Special Issue. Emergent phenomena in quantum many-body systems. *Entropy*, 2025.

[30] John von Neumann. *Mathematical Foundations of Quantum Mechanics*. Princeton University Press, 1955. Originally published in German, 1932, as "Mathematische Grundlagen der Quantenmechanik".

[31] N. J. Cerf and C. Adami. Negative entropy and information in quantum mechanics. *Physical Review Letters*, 79(26):5194–5197, 1997.

[32] Ryszard Horodecki and Paweł Horodecki. —. *Physics Letters A*, 194:147–152, 1994.

[33] Ryszard Horodecki, Paweł Horodecki, and Michał Horodecki. Quantum α-entropy inequalities: independent condition for local separability. *Physics Letters A*, 210(6):377–381, 1996.

[34] C. H. Bennett, D. P. DiVincenzo, J. A. Smolin, and W. K. Wootters. *Phys. Rev. A*, 54:3824, 1996.

[35] M. B. Plenio. *Phys. Rev. Lett.*, 95:090503, 2005.

[36] G. Lindblad. *Commun. Math. Phys.*, 48:119, 1976.

[37] D. A. Turkington. *Generalized Vectorization, Cross-Products, and Matrix Calculus*. Cambridge University Press, Cambridge, 2013.

[38] A. Moharramipour, L. A. Lessa, C. Wang, T. H. Hsieh, and S. Sahu. *arXiv:2406.08542*.

[39] Berislav Buča and Tomaž Prosen. A note on symmetry reductions of the lindblad equation: transport in constrained open spin chains. *New Journal of Physics*, 14(7):073007, 2012.

[40] SciPy Developers. Scipy: Fundamental algorithms for scientific computing in python. https://scipy.org/, 2025. Python package.